SSRG International Journal of Electronics and Communication Engineering
ISSN: 2348-8549/ https://doi.org/10.14445/23488549/IJECE-V13I2P112

Volume 13 Issue 2, 158-165, February 2026

Original Article

Enhanced Iterative Hard Thresholding-Based Cascaded Channel Estimation in IRS-Enabled mmWave MIMO Systems

Poornima Sriramula[1], L. Nirmala Devi[2], A. Nageswar Rao[3]

[1]*Department of Electronics and Communication Engineering, Osmania University, Telangana, India, and School of Engineering, Anurag University, Telangana, India.*
[2]*Department of Electronics and Communication Engineering, Osmania University, Telangana, India.*
[3]*Strategic Electronics Research and Design Center, Hindustan Aeronautics Limited, Telangana, India.*

[1]*Corresponding Author : poornimasriramula2024@gmail.com*

Received: 20 November 2025 Revised: 21 December 2025 Accepted: 22 January 2026 Published: 20 February 2026

Abstract - *The integration of Intelligent Reflecting Surfaces (IRS) with millimeter-Wave (mmWave) Multiple-Input Multiple-Output (MIMO) architectures presents a compelling strategy for improving coverage and boosting spectral efficiency in next-generation wireless systems. A central difficulty in such networks lies in estimating the cascaded channel that incorporates the base station (BS)–IRS and IRS–User Equipment (UE) links. This task is particularly challenging because IRS elements operate passively and lack inherent baseband processing capability. In this work, we introduce an Enhanced Iterative Hard Thresholding (EIHT)–based framework for cascaded channel estimation that is computationally efficient and well-suited for large antenna arrays. By representing the IRS-assisted propagation path in the angular domain, the estimation problem is formulated as a sparse recovery task. The proposed algorithm refines the solution through residual-guided updates using pseudo-inverse projections, eliminating the need for explicit support detection or prior channel statistics. Numerical evaluations show that across a range of SNR levels, the proposed method achieves lower Normalized Mean Square Error (NMSE) and faster convergence than benchmark approaches such as Orthogonal Matching Pursuit (OMP) and classical Iterative Hard Thresholding (IHT). These results position the method as a practical and scalable option for real-time deployment in IRS-enabled mmWave MIMO networks.*

Keywords - *Millimeter Wave, Multiple input multiple output, Intelligent Reflecting Surface, Channel estimation, Iterative Hard Thresholding, Sparse signal recovery.*

1. Introduction

Millimetre wave (mmWave) communication has gained significant attention as a key enabler for high-capacity wireless networks in beyond-5G and future 6G systems, due to its abundant spectrum resources and ability to support extremely high data rates [1, 2]. The availability of large contiguous bandwidths in the mmWave spectrum makes it possible to achieve multi-gigabit-per-second throughput, which is essential for emerging applications such as immersive Virtual Reality (VR), Ultra-High-Definition (UHD) video streaming, autonomous vehicle communication, and massive machine-type communications [3].

However, the deployment of mmWave technology faces substantial challenges. The short wavelength of mmWave signals leads to high free-space path loss and severe sensitivity to physical obstructions such as buildings, vehicles, and foliage. Moreover, mmWave propagation exhibits sparse multipath characteristics, with limited scattering in most practical environments, which further reduces link reliability in Non-Line-of-Sight (NLoS) conditions.

To combat these limitations, hybrid Multiple-Input Multiple-Output (MIMO) architectures have been proposed, combining high-dimensional analog beamforming with low-dimensional digital beamforming [4]. Hybrid beamforming offers a cost-effective and energy-efficient alternative to fully digital architectures by significantly reducing the number of Radio-Frequency (RF) chains. This enables large antenna arrays to achieve high beamforming gains without incurring excessive hardware complexity and power consumption. Nonetheless, the performance of hybrid mmWave MIMO systems deteriorates sharply when the line-of-sight (LoS) link is blocked, and the available reflected or scattered paths are insufficient to maintain reliable connectivity. In dense urban environments, for example, high-rise buildings and other large obstacles frequently disrupt direct transmission paths, leading to coverage holes and degraded quality of service.

Intelligent Reflecting Surfaces (IRS) have recently surfaced as a potential way to circumvent these coverage and reliability problems by reconfiguring the wireless propagation environment [5]. An IRS is a planar array composed of many low-cost passive reflecting components that may independently alter the incident electromagnetic waves' phase and amplitude. By employing a programmable controller, the IRS can dynamically steer reflected signals toward desired receivers, thereby creating virtual LoS links, enhancing received signal strength, and suppressing interference. Unlike conventional amplify-and-forward relays or active repeaters, IRSs operate in a passive manner, reflecting signals without active amplification, frequency conversion, or decoding. This results in minimal hardware cost, negligible additional noise, and very low power consumption, making IRS technology attractive for large-scale deployment in both indoor and outdoor scenarios. Typical installation sites include building façades, billboards, lamp posts, and indoor walls, enabling flexible network planning and coverage enhancement.

Even though IRS-assisted architectures have advantages, integrating them into mmWave MIMO systems presents significant technological obstacles, one of which is the acquisition of accurate Channel State Information (CSI). Accurate prediction of the cascaded channel created by the Base Station (BS)–IRS and IRS–User Equipment (UE) links is essential for efficient beamforming at the base station and appropriate IRS phase shift configuration in IRS-assisted systems. Because IRS elements lack active RF chains and function passively, they are unable to transmit or analyze pilot signals, making this estimation problem intrinsically challenging. Additionally, the number of antennas at the BS and UE, as well as the number of IRS elements, increases the dimensionality of the cascaded channel. Conventional CE methods are therefore unsuited for large-scale IRS-assisted systems due to their high computing complexity and considerable pilot overhead. The goal of obtaining high spectral efficiency is in conflict with traditional estimating techniques like Least Squares (LS), Minimum Mean Square Error (MMSE), and two-stage estimation frameworks, which usually require a large number of training symbols.

To address these challenges, Compressed Sensing (CS) techniques have been extensively explored for mmWave CE by leveraging the inherent angular-domain sparsity of mmWave channels. Representative algorithms, including Orthogonal Matching Pursuit (OMP) [6], basis pursuit [7], and sparse Bayesian learning (SBL) [8], aim to recover sparse channel representations using a reduced number of pilot measurements. Although these methods can effectively reduce training overhead, their computational complexity increases rapidly with system dimensionality. Moreover, their performance is sensitive to noise and angular grid mismatch, which often leads to performance degradation in practical implementations. Most CS-based methods also rely on carefully selected regularization parameters to balance sparsity and reconstruction accuracy, which may require prior knowledge of noise statistics that may not be readily available. A recently proposed online sparse channel estimation method based on an exponentially weighted forgetting-factor LMS has been developed for IRS-assisted mmWave hybrid MIMO systems [9]. This approach provides an effective alternative for addressing the limited signal processing capabilities of IRS elements.

The limitations of existing approaches indicate that current cascaded CE techniques either involve high computational complexity or exhibit slow convergence, particularly in large-scale IRS-assisted systems. Moreover, many of these methods rely on explicit support selection or prior statistical knowledge, which limits their robustness in practical deployment scenarios. To address these shortcomings, a cascaded CE framework based on an Enhanced Iterative Hard Thresholding (EIHT) algorithm is developed in this work. The proposed approach models the IRS-assisted channel in the angular domain and incorporates a residual-based pseudo-inverse update strategy [10] to improve convergence speed and estimation accuracy. Unlike conventional CS-based algorithms, the EIHT framework avoids explicit support identification and does not require prior channel statistics, making it robust to grid mismatch and scalable to large antenna and IRS configurations. The suggested approach delivers accurate CE with less computing complexity and pilot overhead by taking advantage of the sparse structure of mmWave channels.

The following is a summary of this paper's major contributions:

- For IRS-assisted hybrid mmWave MIMO systems, an angular-domain cascaded CE framework is created, taking advantage of channel sparsity to lower training overhead.
- An enhanced iterative hard thresholding algorithm with pseudo-inverse-based residual updates is proposed to accelerate convergence while avoiding the complexity associated with conventional support selection methods.
- Simulation results demonstrate that the proposed approach outperforms existing approaches, such as OMP and traditional IHT, in terms of convergence speed and Normalized Mean Square Error (NMSE), particularly when the Signal-to-Noise Ratio (SNR) is low.

This is how the rest of the paper is structured. The system model for the IRS-assisted mmWave MIMO link is shown in Section 2. The suggested EIHT-based CE technique is presented in Section 3. Computational complexity and convergence behaviour are covered in Section 4. Simulation results and a comparative performance analysis are presented in Section 5. The work is finally concluded in Section 6, which also suggests future research topics.

Notations: Column vectors are represented by lowercase bold letters, and matrices are shown by uppercase bold letters. The complex conjugation, transpose, Hermitian transpose, matrix inverse, and Moore–Penrose pseudo-inverse are represented by the operators, $(.)^*$, $(.)^T$, $(.)^H$, $(.)^{-1}$, $(.)^\dagger$ respectively. The $\mathrm{N} \times \mathrm{N}$ identity matrix is represented by the sign $\boldsymbol{I}_N$. The symbols for the Kronecker product, Khatri-Rao product, and Hadamard product are $\otimes$, $\odot$, $\circ$ respectively. The vectorization of matrix $\boldsymbol{A}$ is indicated by the operator $vec(\boldsymbol{A})$ which is produced by stacking its columns into a single vector.

2. System Model

The hybrid mmWave MIMO communication system with IRS assistance is described in this section. The corresponding cascaded CE problem is then expressed as a sparse recovery task within a Compressed Sensing (CS) framework, enabling effective utilization of the angular-domain sparsity inherent in mmWave channels while reducing training overhead.

2.1. IRS Assisted Hybrid MIMO System

An IRS is used to facilitate communication between a Base Station (BS) and User Equipment (UE) in a downlink transmission scenario. The UE used N_U antennas, whereas the BS has $\mathrm{N_B}$ antennas. Each of the IRS's M passive reflecting elements, which are grouped in a Uniform Planar Array (UPA), has the ability to change the incident electromagnetic signal's phase. It is assumed that the IRS is located on a building façade in the BS's Line-of-Sight (LoS) area. Adaptive reflection to improve link quality is made possible by a dedicated smart controller that configures the IRS phase shifts depending on control information obtained from the BS via a low-rate backhaul link. The channel matrix between the BS and IRS is represented by $H_{BI} \in \mathbb{C}^{\mathrm{M}\times\mathrm{N_B}}$ whereas the channel from the IRS to the UE is represented by $H_{IU} \in \mathbb{C}^{N_U\times\mathrm{M}}$. $M = M_X \times M_Y$ passive reflecting elements form the IRS. As is frequently assumed in mmWave propagation conditions, the direct BS-to-UE communication channel is often disregarded, presuming it is either highly attenuated or completely obstructed by obstacles. The cascaded BS–IRS–UE channel that results can be written as

$$H = H_{IU}\Theta H_{BI} \, , \tag{1}$$

Where, $H \in \mathbb{C}^{N_U\times\mathrm{N_B}}$ denotes the effective end-to-end channel matrix. The diagonal matrix $\Theta \in \mathbb{C}^{\mathrm{M}\times\mathrm{M}}$ represents the IRS reflection coefficients and is given by

$$\Theta = \, diag\{r_1e^{j\theta_1}, r_2e^{j\theta_2}, \ldots, r_Me^{j\theta_M}\}$$

Where $r_m \in [0,1]$ is the associated amplitude reflection coefficient and $\theta_m \in [0,2\pi)$ is the phase shift applied by the m^{th} reflecting element. All IRS elements are considered to have a uniform amplitude, $r_m = 1$ for analytical simplicity.

When compared to fully digital arrays, the hybrid architecture greatly lowers hardware costs at the transceiver side by utilizing both analog and digital beamforming at the BS and UE. The hybrid beamforming framework connects a reduced set of Radio-Frequency (RF) chains to a large-scale antenna array via analog phase-control networks. This approach enables high-dimensional beam steering while lowering hardware complexity and power consumption relative to fully digital architectures. Such a configuration is particularly advantageous in mmWave systems, where the short wavelength allows dense antenna deployment but necessitates highly directional transmissions to achieve sufficient beamforming gain. transmissions.

For channel estimation, the BS transmits T pilot beam patterns sequentially, where the t^{th} beamforming vector is denoted as $f_t \in \mathbb{C}^{N_B\times 1}$. At the UE, each received training signal is processed through a combining vector $w_t \in \mathbb{C}^{N_U\times 1}$. Let x_t denote the pilot symbol transmitted during the t^{th} training interval. The received signal can be compactly recorded in matrix form by stacking the observations corresponding to all T pilot transmissions as

$$Y = W^H HFX + N \tag{2}$$

Where $Y \in \mathbb{C}^{\mathrm{T}\times\mathrm{T}}$ denotes the received signal matrix, $W \in \mathbb{C}^{N_U\times\mathrm{T}}$ represents the combining matrix formed from the UE combining vectors, and $F \in \mathbb{C}^{N_B\times\mathrm{T}}$ denotes the beamforming matrix constructed from the BS precoding vectors. The pilot matrix $X \in \mathbb{C}^{T\times\mathrm{T}}$ is defined as a diagonal matrix whose diagonal entries correspond to the transmitted pilot symbols x_t. For analytical convenience, the pilot matrix is selected as $X = \sqrt{P}\, I_T$, where P denotes the pilot transmission power. Independent, identically distributed complex Gaussian noise samples with zero mean and variance σ_n^2 are included in the matrix $N \in \mathbb{C}^{T\times\mathrm{T}}$.

At the BS, hybrid precoding is employed, where the overall precoder $F = F_{RF}F_{BB}$, consists of an analog RF precoder $F_{RF} \in \mathbb{C}^{N_B\times N_\mathrm{B}}$ implemented using phase shifter networks, followed by a digital baseband precoder $F_{BB} \in \mathbb{C}^{N_B\times\mathrm{T}}$. In a similar manner, the UE adopts a hybrid combining structure given by $W = W_{RF}W_{BB}$, where $W_{RF} \in \mathbb{C}^{N_U\times\mathrm{N}_U}$ denotes the analog combine and $W_{BB} \in \mathbb{C}^{N_U\times\mathrm{T}}$ represents the digital baseband combining matrix. The received signal matrix may be rewritten as follows by substituting the cascaded channel expression (1) into (2), as shown.

$$Y = \sqrt{P} W^H H_{IU}\Theta H_{BI}F + N \tag{3}$$

For the IRS-assisted mmWave MIMO system under consideration, (3) yields the mathematical representation of the received training signal, which forms the foundation for the channel modelling discussed in the subsequent section.

2.2. IRS Assisted mmWave MIMO Channel Model

In the IRS-assisted mmWave MIMO system under discussion, the propagation links between the Base Station (BS) and the IRS, as well as between the IRS and the User Equipment (UE), are characterized using a geometric channel model that captures the underlying multipath propagation behavior of the wireless environment. Due to the high-frequency nature of mmWave signals, only a few numbers of dominant propagation paths contribute significantly to the channel response. Thus, the sparse multipath structure of the underlying wireless environment is successfully represented by modelling the BS–IRS and IRS–UE channels using the L and L' dominant paths, respectively.

The channel, represented by H_{BI}, between the BS and the IRS is written as

$$H_{BI} = \sqrt{\frac{N_B M}{L}} \sum_{l=1}^{L} \alpha_l a_I(\theta_l, \phi_l) a_B^H(\psi_l) \tag{4}$$

where the complex gain is connected to the l^{th} propagation channel is represented by $\alpha_l \sim CN(0, \sigma_\alpha^2)$. The BS array response for the angle of departure (AoD) ψ_l is represented by the vector $a_B(\psi_l)$, whereas the IRS array response vector is associated with the elevation angle θ_l and azimuth angle ϕ_l for the l^{th} path is represented by the vector $a_I(\theta_l, \phi_l)$.

An identical geometric formulation can also be used to define the channel between the IRS and the UE, represented by H_{IU}.

$$H_{IU} = \sqrt{\frac{N_U M}{L'}} \sum_{l'=1}^{L'} \beta_{l'} a_U(\psi_{l'}) a_I^H(\theta_{l'}, \phi_{l'}) \tag{5}$$

Where the complex gain of the l'^{th} propagation path is represented by $\beta_{l'} \sim CN(0, \sigma_\beta^2)$. The UE array response for the angle of arrival (AoA) $\psi_{l'}$ is represented by the vector $a_U(\psi_{l'})$, whereas the IRS array response for the elevation angle $\theta_{l'}$ and azimuth angle $\phi_{l'}$ of the l'^{th} path is represented by $a_I(\theta_{l'}, \phi_{l'})$. While the IRS is set up as a Uniform Rectangular Array (URA) with $M = M_X M_Y$ reflecting elements, the BS and UE are assumed to employ uniform linear arrays.

For the BS and UE equipped with ULAs comprising N_B and N_U antenna elements, respectively, and assuming an inter-element spacing $d = \lambda/2$, the corresponding array response vectors are given by

$$\boldsymbol{a}_B(\psi_l) = \frac{1}{\sqrt{N_B}} \left[1, e^{\frac{j2\pi d \cos(\psi_l)}{\lambda}}, \cdots, e^{\frac{j2\pi d (N_B-1)\cos(\psi_l)}{\lambda}}\right]^T$$

$$\boldsymbol{a}_U(\psi_{l'}) = \frac{1}{\sqrt{N_U}} \left[1, e^{\frac{j2\pi d \cos(\psi_{l'})}{\lambda}}, \cdots, e^{\frac{j2\pi d (N_U-1)\cos(\psi_{l'})}{\lambda}}\right]^T$$

A URA with dimensions $M_X \times M_Y$, is used to model the IRS. The Kronecker product of the horizontal and vertical steering vectors yields the appropriate IRS array response vector, which is represented as

$$\boldsymbol{a}_I(\theta_l, \phi_l) = \boldsymbol{a}_x(\theta_l, \phi_l)\boldsymbol{a}_y(\phi_l)$$
$$\boldsymbol{a}_I(\theta_{l'}, \phi_{l'}) = \boldsymbol{a}_x(\theta_{l'}, \phi_{l'})\boldsymbol{a}_y(\phi_{l'})$$

The horizontal and vertical array response components associated with the l^{th} path is defined as

$$\boldsymbol{a}_x(\theta_l, \phi_l) = \frac{1}{\sqrt{M_x}} \left[1, e^{\frac{j2\pi d \sin(\phi_l)\cos(\theta_l)}{\lambda}}, \cdots, e^{\frac{j2\pi d (M_x-1)\sin(\phi_l)\cos(\theta_l)}{\lambda}}\right]^T$$
$$\boldsymbol{a}_y(\phi_l) = \frac{1}{\sqrt{M_y}} \left[1, e^{\frac{j2\pi d \cos(\phi_l)}{\lambda}}, \cdots, e^{\frac{j2\pi d (M_y-1)\cos(\phi_l)}{\lambda}}\right]^T$$

Similarly, for the l^{th} path, the horizontal and vertical vectors are given by

$$\boldsymbol{a}_x(\theta_{l'}, \phi_{l'}) = \frac{1}{\sqrt{M_x}} \left[1, e^{\frac{j2\pi d \sin(\phi_{l'})\cos(\theta_{l'})}{\lambda}}, \cdots, e^{\frac{j2\pi d (M_x-1)\sin(\phi_{l'})\cos(\theta_{l'})}{\lambda}}\right]^T$$
$$\boldsymbol{a}_y(\phi_{l'}) = \frac{1}{\sqrt{M_y}} \left[1, e^{\frac{j2\pi d \cos(\phi_{l'})}{\lambda}}, \cdots, e^{\frac{j2\pi d (M_y-1)\cos(\phi_{l'})}{\lambda}}\right]^T$$

3. Problem Formulation

The goal of this study is to estimate the downlink cascaded channel related to the mmWave MIMO system with the IRS-assistance that was described in the previous section. The cascaded CE task is reduced to finding the Angles of Departure (AoDs), Angles of Arrivals (AoAs), and the accompanying complex path gains for the BS–IRS and IRS–UE links based on the chosen geometric channel model. The resultant channel shows sparsity when depicted in the angular domain because mmWave propagation is dominated by a small number of significant paths. This characteristic makes it possible to naturally formulate the cascaded CE issue in a Compressed Sensing (CS) framework as a sparse signal recovery challenge.

3.1. Preliminaries

Within the CS framework, an unknown signal vector $\boldsymbol{x} \in \mathbb{C}^N$ is observed through a linear measurement process of the form

$$y = \Phi x + n$$

Where $\Phi \in \mathbb{C}^{M\times N}$ denotes the sensing matrix, $y \in \mathbb{C}^{M}$ represents the measurement vector, and $n \in \mathbb{C}^{M}$ corresponds to additive noise. Typically, the number of measurements satisfies $M < N$, rendering the system underdetermined. To recover x, prior knowledge about its sparsity is used. Specifically, if x admits a sparse representation over a dictionary Ψ, it can be expressed as

$$x = \Psi s$$

Where the coefficient vector s contains only K nonzero entries, with $K \ll N$. Substituting this representation into the measurement model yields

$$y = \Phi\Psi s + n$$

Recovery of the sparse coefficient vector s can be formulated as

$$\hat{s} = arg\min_{s} \|s\|_0 \ subject\ to\ \|y - \Phi\Psi s\|_2 \le \epsilon$$

Where ϵ denotes a tolerance parameter that accounts for measurement noise. Directly solving the above ℓ_0- norm minimization problem is computationally intractable due to its combinatorial nature. Consequently, various approximation and relaxation techniques have been developed to enable practical sparse signal recovery.

Among these, thresholding-based greedy algorithms have attracted significant interest due to their capacity for iterative refinement and low computational complexity. In particular, Iterative Hard Thresholding (IHT) methods update the signal estimate by alternately performing gradient-based corrections and enforcing sparsity through hard thresholding. Such approaches are especially appealing for mmWave MIMO channel estimation, where the underlying channel structure is inherently sparse, and the available pilot resources are limited. Compared to convex relaxation techniques such as basis pursuit, greedy thresholding methods typically offer reduced computational complexity and faster convergence, making them suitable for large-scale systems with constrained measurement budgets.

3.2. Sparse Formulation of mmWave Channel

The channels associated with the BS–IRS and IRS–UE links show sparsity when observed in the angular domain due to the restricted scattering nature of mmWave propagation. To exploit this property, the cascaded channel is expressed using overcomplete angular dictionaries constructed from array response vectors corresponding to discretized angular grids. In particular, the BS–IRS channel matrix may be represented as

$$H_{BI} = A_I \Lambda_\alpha A_B^H \tag{5}$$

The IRS to UE channel is written as,

$$H_{IU} = A_U \Lambda_\beta A_I^H \tag{6}$$

Here, $A_I \in \mathbb{C}^{M\times G_I}$, $A_U \in \mathbb{C}^{N_U\times G_U}$, and $A_B \in \mathbb{C}^{N_B\times G_B}$, denote the angular dictionary matrices associated with the IRS and BS, respectively. Each column of these matrices corresponds to an array response vector evaluated at a quantized angle from the predefined angular grid. The dictionary matrices are constructed as

$$A_B = \left[a_B(\psi_1), a_B(\psi_2), \dots, a_B\left(\psi_{G_B}\right)\right]$$
$$A_U = \left[a_U(\psi_1), a_U(\psi_2), \dots, a_U\left(\psi_{G_U}\right)\right]$$
$$A_x = \left[a_x(\theta_1, \phi_1), a_x(\theta_2, \phi_2), \dots, a_x\left(\theta_{G_x}, \phi_{G_x}\right)\right]$$
$$A_y = \left[a_y(\phi_1), a_y(\phi_2), \dots, a_y\left(\phi_{G_y}\right)\right]$$
$$A_I = A_x \otimes A_y$$

The angular domains associated with the BS, UE, and IRS are uniformly quantized into discrete grids, where the BS and UE angular ranges are $[0, \pi]$ are divided into G_B and G_U bins, respectively, while the IRS azimuth and elevation domains $[0, 2\pi)$ and $[0, \pi]$ are discretized into G_x and G_y bins, such that the total angular resolution is given by $G_I = G_x G_y$. The coefficient matrices $\Lambda_\alpha \in \mathbb{C}^{G_I\times G_B}$ and $\Lambda_\beta \in \mathbb{C}^{G_U\times G_I}$ exhibit sparse, containing only L and L' nonzero elements, respectively, which correspond to the effective complex path gains α_l and $\beta_{l'}$ associated with the IRS-BS and UE-IRS propagation links.

The measurement equation may be rewritten as follows by replacing the received signal model in (3) with the sparse angular-domain representations in (5) and (6).

$$Y = \sqrt{P} W^H A_U \Lambda_\beta A_I^H \Theta A_I \Lambda_\alpha A_B^H F + N \tag{7}$$

By applying the vectorization operator, which arranges the columns of Y into a single vector, we obtain

$$\begin{aligned} y &= vec(Y) \\ &= vec\left(\sqrt{P} W^H A_U \Lambda_\beta A_I^H \Theta A_I \Lambda_\alpha A_B^H F + N\right) \\ &= (F^T \otimes W^H)\, vec(A_U \Lambda_\beta A_I^H \Theta A_I \Lambda_\alpha A_B^H) + vec(N) \\ &= (F^T \otimes W^H)(A_B^* \otimes A_U) vec(\Lambda_\beta A_I^H \Theta A_I \Lambda_\alpha) + n \\ &= (F^T \otimes W^H)\,(A_B^* \otimes A_U)\left(\Lambda_\alpha^T \otimes \Lambda_\beta\right) vec(A_I^H \Theta A_I) + n \\ &= (F^T \otimes W^H)\,(A_B^* \otimes A_U)\left(\Lambda_\alpha^T \otimes \Lambda_\beta\right)(A_I^* \odot A_I)\, vecd(\Theta) \\ &\quad + n \end{aligned} \tag{8}$$

To simplify the above expression, we utilize the structural property of the IRS dictionary matrix A_I . For the k^{th} column $a_k \in \mathbb{C}^{M\times 1}$ of A_I , it holds that

$$A_I^T \circ \left(a_k^H \otimes 1_{G_I}\right) = P_k A_I^T$$

Where the rows of A_I are rearranged by the permutation matrix $P_k \in \mathbb{C}^{G_I \times G_I}$. Using this property, the term in (8), i.e.,

$$\left(\Lambda_\alpha^T \otimes \Lambda_\beta\right)\left(A_I^* \odot A_I\right)$$

can be expressed as

$$\left(\Lambda_\alpha^T \otimes \Lambda_\beta\right)\left(A_I^* \odot A_I\right) = \left(\sum_{k=1}^{G_I} \left(\Lambda_k^T \otimes \Lambda_\beta\right) P_k\right) A_I^T = \hat{\Lambda} A_I^T$$

Where $\Lambda_k \in \mathbb{C}^{G_B \times 1}$ represents the k^{th} column of Λ_α^T, while $\hat{\Lambda} \in \mathbb{C}^{G_B G_U \times G_I}$ denotes a sparse matrix that contains only LL' nonzero entries corresponding to the effective propagation paths.

Substituting this into (8), the received signal model, we obtain

$$\begin{aligned} y &= (F^T \otimes W^H)(A_B^* \otimes A_U)\, \hat{\Lambda} A_I^T\, vecd(\Theta) + n \\ &= (F^T \otimes W^H)(A_B^* \otimes A_U)\, \hat{\Lambda} A_I^T \mathfrak{z} + n \\ &= \left(\mathfrak{z}^T A_I \otimes (F^T \otimes W^H)(A_B^* \otimes A_U)\right) vec(\hat{\Lambda}) + n \\ &= \left(\mathfrak{z}^T A_I \otimes (F^T \otimes W^H)(A_B^* \otimes A_U)\right) h_b + n \\ &= Q_{bar} h_b + n \end{aligned}$$

Where $\mathfrak{z} = vecd(\Theta) \in \mathbb{C}^{M \times 1}$ it is the vector of IRS reflection coefficients obtained from the diagonal entries of the IRS phase shift matrix Θ, $h_b = vec(\hat{\Lambda}) \in \mathbb{C}^{G_B G_U G_I \times 1}$ represents the angular-domain sparse representation of the cascaded BS–IRS–UE channel, containing LL' nonzero components, while Q_{bar} denotes the corresponding effective sensing matrix, which is defined as

$$Q_{bar} = \mathfrak{z}^T A_I \otimes (F^T \otimes W^H)(A_B^* \otimes A_U) \in \mathbb{C}^{T^2 \times G_B G_U G_I}$$

To enable efficient channel recovery with reduced computational complexity, the proposed EIHT algorithm is employed to estimate the sparse vector h_b. Once h_b, is obtained, he cascaded channel can be reconstructed as

$$\widehat{H} = (A_B^* \otimes A_U)\, \widehat{H}_b\, A_I^T \mathfrak{z}$$

Where h_b is rephrased into a $G_B G_U \times G_I$ matrix to create $\widehat{H}_b$.

3.3. Sparse Cascaded Channel Identification Using EIHT in IRS-Enabled mmWave Systems

An Enhanced Iterative Hard Thresholding (EIHT) algorithm that exploits the sparsity of the channel representation in the angular domain is used to efficiently recover the cascaded BS–IRS–UE channel.

This formulation allows for the expression of the CE problem in a compressed sensing framework as

$$y = Q_{bar} h_b + n$$

Where h_b is the cascaded channels sparse angular-domain representation, n is the additive noise vector, and Q_{bar} is the effective sensing matrix. The objective is to accurately recover h_b from noisy and underdetermined measurements while maintaining low computational complexity.

Unlike conventional greedy approaches such as OMP, which sequentially identify support indices, or standard IHT, which relies only on gradient-type updates, the EIHT algorithm integrates the pseudo-inverse of the sensing matrix in its update step. This pseudo-inverse projection provides a more stable correction direction, especially when the sensing matrix is highly coherent or ill-conditioned. The iteration proceeds by first computing the residual between the received measurements and the current estimate, then projecting this residual through $Q_{bar}{}^{\dagger}$, and finally applying a hard thresholding operator that retains only the LL' largest entries in magnitude. This step explicitly enforces the known sparsity level of the channel, thereby accelerating convergence and avoiding the spread of energy over irrelevant components.

Algorithm 1: EIHT for IRS-Assisted Channel Estimation

Input:	measurement vector y, sensing matrix Q_{bar}, sparsity level L, step size λ, tolerance δ, maximum iterations T_{max}
Initialization:	$h_b^{(0)} = 0, k = 0$
Repeat:	
1. Compute residual:	$r^{(k)} = y - Q_{bar} h_b^{(k)}$
2. Update estimate:	$u^{(k)} = h_b^{(k)} - \lambda Q_{bar}{}^{\dagger} r^{(k)}$
3. Support selection:	Identify indices of the L largest entries of $u^{(k)}$
4. Hard thresholding:	retain coefficients on the selected support and set all others to zero.
5. Check stopping rule	If $\left\lVert Q_{bar}(h_b^{(k-1)} - h_b^{(k)})\right\rVert_2 \le \delta$ or $k \ge T_{max}$
Output:	Final sparse estimate h_b, reshaped into beamspace channel, H

The above algorithm 1 describes the EIHT process. The algorithm is initialized with $\boldsymbol{h}_b = 0$ and iteratively updated until either the relative difference between consecutive estimates falls below a predefined tolerance or a maximum iteration limit is reached.

Upon termination, the recovered sparse vector is reshaped into the beamspace channel matrix, which is subsequently used to reconstruct the cascaded channel through the corresponding dictionary matrices of the BS, IRS, and UE.

The three operations performed in each iteration of the suggested EIHT algorithm largely determine its computational complexity. First, the multiplication of the effective sensing matrix $Q_{bar} \in \mathbb{C}^{T^2 \times G_B G_U G_I}$ with the sparse vector $h_b \in \mathbb{C}^{G_B G_U G_I \times 1}$ incurs a computational cost of $O(T^2 G_B G_U G_I)$. Second, the pseudo-inverse-based update $\lambda Q_{bar}{}^{\dagger} r$, where $r = y - Q_{bar} h_b$, introduces an additional complexity of the same order, namely $O(T^2 G_B G_U G_I)$. Third, the hard-thresholding operation, which retains the L dominant elements of h_b can be implemented using partial sorting with complexity $O(G_B G_U G_I \log L)$. Because of this, the EIHT algorithms' per-iteration computational complexity is reasonable and comparable to that of greedy approaches such as Orthogonal Matching Pursuit (OMP). Moreover, the improved numerical stability of EIHT under coherent training conditions makes it well-suited for scalable, real-time CE in IRS-assisted mmWave MIMO systems.

4. Results and Discussion

This section evaluates the performance of the proposed CE approach through numerical simulations conducted under various system configurations. The transceiver is equipped $N_B = N_U = 32$ antennas at both the UE and BE, $N_B^{RF} = N_U^{RF} = 8$ number of RF chains to support hybrid precoding and combining. The IRS comprised $M = 8 \times 8$ passive reflecting elements. The propagation environment assumed four dominant multipath components with L$= 2, L' = 2$. Angular resolution was modeled with $G_x = G_y = 7$ along the

Table 1. Numerical comparison of OMP, IHT, and EIHT for IRS-assisted mmWave channel estimation

Metric	OMP	IHT	EIHT
NMSE (5dB)	2.2489	2.1045	-4.1682
NMSE (-5dB)	11.8796	3.6425	-3.3934
NMSE (20 Iterations)	7.7546	-0.5362	-2.2650
Convergence Speed	Slow	Moderate	Fast
SE(5dB) bps/Hz	8.3575	9.1476	10.1221

Horizontal and vertical axes, and the grid sizes at the UE, IRS, and BS were set to $G_U = G_I = G_B = 49$ respectively. CE accuracy is evaluated using the Normalized Mean Squared Error (NMSE), defined as

$$\mathbb{E}\left\{\frac{\left\|\boldsymbol{H} - \widehat{\boldsymbol{H}}\right\|_F^2}{\|H\|_F^2}\right\}$$

While the Spectral Efficiency (SE) metric is employed to assess overall system performance, the performance of the proposed EIHT-based estimator is examined through comparisons with widely used baseline methods, including OMP and IHT algorithms.

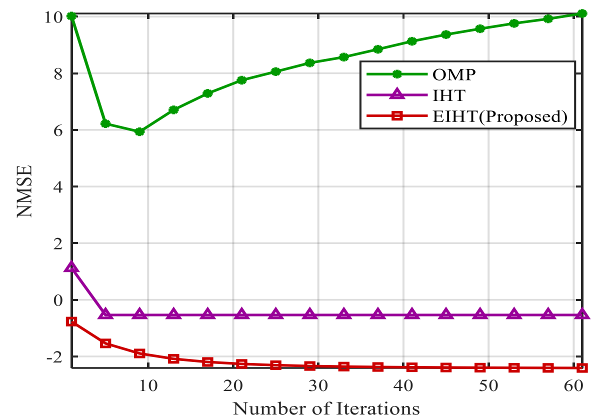

Fig. 1 NMSE performance as a function of iterations for different channel estimation algorithms

Figure 1 displays the NMSE performance as a function of the number of iterations. The findings demonstrate that the suggested EIHT algorithm converges more rapidly and attains a lower steady-state NMSE than both OMP and conventional IHT. The relatively poor convergence of OMP can be attributed to its sensitivity to the stopping criteria and the structure of the equivalent sensing matrix, both of which limit its estimation accuracy. The NMSE performance is shown against the Signal-to-Noise Ratio (SNR) in Figure 2. With increasing SNR, all considered algorithms exhibit improved estimation accuracy. However, the proposed EIHT approach consistently achieves lower NMSE across the entire SNR range. At an SNR of -5 dB, OMP, IHT, and EIHT attain NMSE values on the order reported in the figure, with EIHT providing the most accurate estimate. Overall, the results demonstrate that EIHT achieves nearly an order-of-magnitude reduction in NMSE compared with OMP and approximately a two-fold improvement over conventional IHT. Figure 3 illustrates the corresponding Spectral Efficiency (SE) performance versus SNR. As CE accuracy improves at higher SNR levels, a corresponding increase in SE is observed for all methods. In the high-SNR regime (>0 dB), the proposed EIHT-based estimator offers a pronounced advantage, achieving higher SE than OMP and IHT.

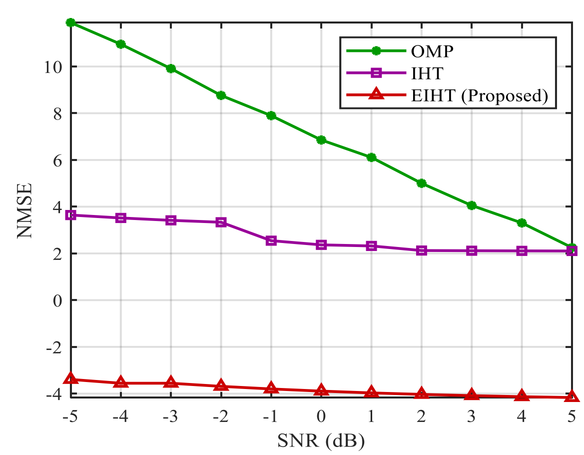

Fig. 2 NMSE versus SNR for different channel estimation algorithms

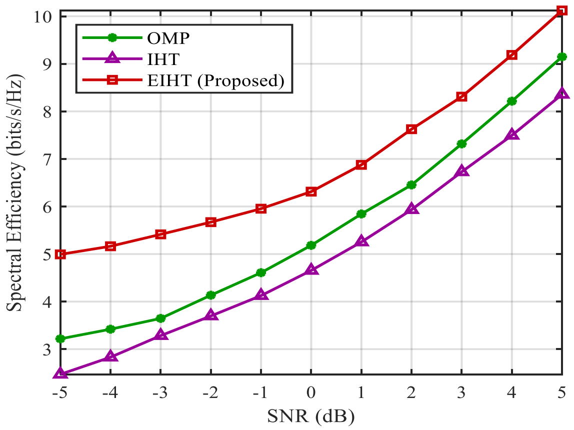

Fig. 3 SE performance as a function of SNR under different estimation schemes

In terms of NMSE and SE under typical operating conditions, Table 1 presents a comparative review of the channel estimation technique under consideration. The table reports NMSE performance at -5 dB and 5 dB, highlighting the robustness of each method. In addition, NMSE values after 20 iterations are presented to illustrate the convergence behavior and estimation stability of the algorithms. To evaluate the effect of channel estimation accuracy on overall system performance, the spectral efficiency attained at an SNR of 5 dB is also presented. From the comparison, it can be observed that the proposed approach consistently achieves lower NMSE and higher spectral efficiency than the benchmark methods, demonstrating its effectiveness in balancing estimation accuracy, convergence efficiency, and achievable data rates under practical mmWave operating conditions.

Overall, these results indicate that the EIHT algorithm achieves superior CE accuracy and SE compared with existing techniques, while maintaining significantly lower computational complexity and better stability than greedy estimators like OMP. Hence, EIHT emerges as a practical and effective solution for real-time CE in IRS-assisted mmWave MIMO systems.

5. Conclusion

In this study, an Efficient Iterative Hard Thresholding (EIHT) algorithm was proposed for CE in IRS-assisted mmWave MIMO systems by formulating the cascaded BS–IRS–UE channel within a compressed sensing framework. The proposed method exploits angular-domain sparsity and employs a pseudo-inverse-based update combined with hard thresholding to achieve accurate and robust recovery with reduced computational burden. Simulation results validated that EIHT outperforms conventional greedy methods in terms of normalized mean square error and convergence speed, particularly under low-to-moderate SNR conditions. Owing to its low complexity and stability, the proposed algorithm is well-suited for real-time IRS-aided mmWave systems, with potential extensions toward wideband and mobility-aware scenarios.

References

[1] Theodore S. Rappaport et al., “Wireless Communications and Applications above 100 GHz: Opportunities and Challenges for 6G and Beyond,” *IEEE Access*, vol. 7, pp. 78729-78757, 2019. [CrossRef] [Google Scholar] [Publisher Link]

[2] Harsh Tataria et al., “6G Wireless Systems: Vision, Requirements, Challenges, Insights, and Opportunities,” *Proceedings of the IEEE*, vol. 109, no. 7, pp. 1166-1199, 2021. [CrossRef] [Google Scholar] [Publisher Link]

[3] Thorsten Wild, Volker Braun, and Harish Viswanathan, “Joint Design of Communication and Sensing for Beyond 5G and 6G Systems,” *IEEE Access*, vol. 9, pp. 30845-30857, 2021. [CrossRef] [Google Scholar] [Publisher Link]

[4] Wei Hong et al., “The Role of Millimeter-Wave Technologies in 5G/6G Wireless Communications,” *IEEE Journal of Microwaves*, vol. 1, no. 1, pp. 101-122, 2021. [CrossRef] [Google Scholar] [Publisher Link]

[5] Wei Wang, and Wei Zhang, “Joint Beam Training and Positioning for Intelligent Reflecting Surfaces Assisted Millimeter Wave Communications,” *IEEE Transactions on Wireless Communications*, vol. 20, no. 10, pp. 6282-6297, 2021. [CrossRef] [Google Scholar] [Publisher Link]

[6] Tian Lin et al., “Channel Estimation for IRS-Assisted Millimeter-Wave MIMO Systems: Sparsity-Inspired Approaches,” *IEEE Transactions on Communications*, vol. 70, no. 6, pp. 4078-4092, 2022. [CrossRef] [Google Scholar] [Publisher Link]

[7] Xiaoling Hu, Rui Zhang, and Caijun Zhong, “Semi-Passive Elements Assisted Channel Estimation for Intelligent Reflecting Surface-Aided Communications,” *IEEE Transactions on Wireless Communications*, vol. 21, no. 2, pp. 1132-1142, 2022. [CrossRef] [Google Scholar] [Publisher Link]

[8] Wuqiong Zhao et al., “OMPL-SBL Algorithm for Intelligent Reflecting Surface-Aided mmWave Channel Estimation,” *IEEE Transactions on Vehicular Technology*, vol. 72, no. 11, pp. 15121-15126, 2023. [CrossRef] [Google Scholar] [Publisher Link]

[9] Vidya Bhasker Shukla, Vimal Bhatia, and Kwonhue Choi, “Cascaded Channel Estimator for IRS-Aided mmWave Hybrid MIMO System,” *IEEE Wireless Communications Letters*, vol. 13, no. 3, pp. 622-626, 2024. [CrossRef] [Google Scholar] [Publisher Link]

[10] Jinming Wen et al., “A Pseudo-Inverse-Based Hard Thresholding Algorithm for Sparse Signal Recovery,” *IEEE Transactions on Intelligent Transportation Systems*, vol. 24, no. 7, pp. 7621-7630, 2023. [CrossRef] [Google Scholar] [Publisher Link]